Photosynth Res
DOI 10.1007/s11120-008-9398-7

REGULAR PAPER

Towards efficient hydrogen production: the impact of antenna size and external factors on electron transport dynamics in *Synechocystis* PCC 6803

Gábor Bernát · Nadine Waschewski · Matthias Rögner

Received: 11 April 2008 / Accepted: 23 December 2008

Abstract Three *Synechocystis* PCC 6803 strains with different levels of phycobilisome antenna-deficiency have been investigated for their impact on photosynthetic electron transport and response to environmental factors (i.e. light-quality, -quantity and composition of growth media). Oxygen yield and P_{700} reduction kinetic measurements showed enhanced linear electron transport rates—especially under photoautotrophic conditions—with impaired antenna-size, starting from wild type (WT) (full antenna) over ΔapcE- (phycobilisomes functionally dissociated) and Olive (lacking phycocyanin) up to the PAL mutant (lacking the whole phycobilisome). In contrast to mixotrophic conditions (up to 80% contribution), cyclic electron transport plays only a minor role (below 10%) under photoautotrophic conditions for all the strains, while linear electron transport increased up to 5.5-fold from WT to PAL mutant. The minor contribution of the cyclic electron transport was proportionally increased with the linear one in the ΔapcE and Olive mutant, but was not altered in the PAL mutant, indicating that upregulation of the linear route does not have to be correlated with downregulation of the cyclic electron transport. Antenna-deficiency involves higher linear electron transport rates by tuning the PS2/PS1 ratio from 1:5 in WT up to 1:1 in the PAL mutant. While state transitions were observed only in the WT and Olive mutant, a further ~30% increase in the PS2/PS1 ratio was achieved in all the strains by long-term adaptation to far red light (720 nm). These results are discussed in the context of using these cells for future H_2 production in direct combination with the photosynthetic electron transport and suggest both Olive and PAL as potential candidates for future manipulations toward this goal. In conclusion, the highest rates can be expected if mutants deficient in phycobilisome antennas are grown under photoautotrophic conditions in combination with uncoupling of electron transport and an illumination which excites preferably PS1.

Keywords Light adaptation · Linear and cyclic electron flow · Photo-biological hydrogen production · Phycobilisomes · *Synechocystis*

Abbreviations

APC	Allophycocyanin
CCCP	Carbonyl-cyanide m-chlorophenylhydrazone
Chl	Chlorophyll
Cyt	Cytochrome
DCBQ	2,6-Dichloro-benzoquinone
DCMU	3-(3′,4′-Dichlorophenyl)-1,1-dimethylurea
FNR	Ferredoxin:$NADP^+$ oxidoreductase
H_2-ase	Hydrogenase
L_{CM}	ApcE, the 99 kDa phycobilisome core-membrane linker protein
MV	Methyl viologen
P_{700}	The primary electron donor of PS1
PBS	Phycobilisome
PC	Phycocyanin
PQ	Plastoquinone
PS	Photosystem
WT	Wild type

Introduction

Although many technical problems still have to be solved, molecular hydrogen is considered to be one of the most

G. Bernát (✉) · N. Waschewski · M. Rögner
Lehrstuhl für Biochemie der Pflanzen, Ruhr Universität Bochum, 44780 Bochum, Germany
e-mail: gabor.bernat@rub.de

Published online: 10 January 2009

promising candidates as future energy carrier. However, one major environmental problem for the realization of a hydrogen-based economy is the fact that present hydrogen production is mainly based on fossil rather than on regenerative technologies. If hydrogen could be produced from renewable resources such as water and light energy, using the biological catalyst photosystem 2 (PS2) for water splitting on the one end and a hydrogenase (H_2-ase) enzyme (for review see Vignais and Billoud 2007) for H_2 production on the other, a circular process without net CO_2 emission could be realized.

To a certain extent, some unicellular photosynthetic organisms (e.g., the green algae *Chlamydomonas reinhardtii* as well as several types of cyanobacteria) perform already such a photobiological process in which these enzymes are functionally linked by the linear photosynthetic electron transport chain, which in turn is energized by sunlight. The drawback of this direct coupling of photosynthesis and hydrogen production is the fact that the hydrogenases of these systems [for review see (Ghirardi et al. 2007)] are extremely oxygen-sensitive. For this reason, strict anaerobic conditions are required, which can be maintained only for a limited time, thereby reducing the potentially high hydrogen evolution to a correspondingly low value (Kruse et al. 2005); for an estimation of the highest potential yield see (Melis and Happe 2001). In order to create an organism with the highest possible rate of photosynthesis-coupled hydrogen formation, highly active hydrogenases have to be engineered for oxygen tolerance, and these hydrogenases then have to be coupled efficiently to an optimized linear photosynthetic electron transport chain [for details see the review by (Esper et al. 2006)]. A promising candidate for such a model organism which has to be simple, easily transformable and well characterized is the cyanobacterium *Synechocystis* PCC 6803. Besides its completely sequenced genome and increasing number of mutants, a specific advantage of *Synechocystis* PCC 6803 is its capability to grow auto-, hetero- or mixotrophically. However, two disadvantageous properties of this organism toward this goal should be eliminated: its low PS2/PS1 ratio and the low activity of its internal H_2-ase, which also operates only under anaerobic conditions. While the oxygen-sensitive hydrogenase has to be replaced by a highly active, engineered heterologous enzyme in the future, the linear photosynthetic electron flow has to be increased considerably under appropriate conditions in order to achieve the highest hydrogen yields. Fortunately, similar to higher plants and green algae (Leong and Anderson 1986; Pfannschmidt et al. 2001), the PS2/PS1 ratio in cyanobacteria can be modulated by factors influencing long-term adaptation processes which optimize photosynthetic efficiency and protect the organism from photodamage. These factors include changes in light quality/quantity and the absence/presence of genes involved directly or indirectly in this regulation. Fujita and coworkers observed a significant increase in the PS2/PS1 ratio when *Synechocystis* PCC 6714 had been cultivated either under far red or strong white light [see the review (Fujita et al. 1994) and references therein] while the PS2/Cytochrome (Cyt) b_6f ratio remained unchanged (Fujita and Murakami 1987; Fujita et al. 1994). It was also shown, that the *Synechocystis* genes *pmgA* and *sll1961* are involved in the modulation of photosystem stoichiometry, but their knock-out would not be beneficial for our purpose since it apparently decreases the PS2/PS1 ratio (Fujimori et al. 2005; Ozaki et al. 2007; Sonoike et al. 2001). In contrast, elevated PS2/PS1 ratios were observed when either the *apcAB* or *cpcG1* genes were knocked out (Ajlani and Vernotte 1998; Kondo et al. 2007, in this issue). These genes encode the phycobilisome (PBS) core and the 27 kDa rod-core linker proteins (L_{RC}^{27}) showing the strong impact of PBS antenna size on the PS2/PS1 ratio.

In this report, we evaluate three *Synechocystis* mutants with different levels of antenna deficiency in comparison with wild type (WT) for being an appropriate starting strain for future engineering photosynthesis-based hydrogen production. These strains involve (a) an apcE-less mutant which lacks the 99 kDa core-membrane linker protein (L_{CM}) resulting in an impaired binding between PBS and photosystems combined with a suppressed energy transfer (Shen et al. 1993), (b) the Olive mutant which lacks phycocyanin (PC) (Rögner et al. 1990) and (c) the PAL mutant which lacks the whole PBS (Ajlani and Vernotte 1998). The objective of this study is an in-depth analysis of these mutants with respect to their linear-to-cyclic electron transport, their energy distribution between the photosystems in short and long term, and their dynamic adaptation to changing environmental conditions such as light composition and growth conditions. This first systematic comparison of antenna-deficient mutants in respect to photosynthetic activity should finally help to select the most appropriate *Synechocystis* strain(s) for further genetic engineering (e.g., insertion of oxygen-resistant foreign H_2-ase etc.) toward efficient photo-biological hydrogen production.

Materials and methods

Cell cultures

Synechocystis ΔapcE and PAL mutants have been designed by Shen and coworkers (Shen et al. 1993) and Ajlani and Vernotte (1998) by deletion of the correspondent *apcE* and *apcAB* operons, respectively. The glucose-tolerant, PC-less Olive mutant was selected by its phenotype (Rögner et al.

1990). Solid stock cultures were kept on agar plates supplemented with 5 mM glucose. To keep the selection pressure, the agar media of PAL and ΔapcE mutants contained 35 μg/ml chloramphenycol and 20 μg/ml erythromycin, respectively. Liquid cultures of WT and mutant cells were routinely grown in standard BG11 media under white fluorescence light of 45–70 μE/m^2s at 30°C, starting with precultures of approx. $OD_{730} = 0.3$. Mixotrophic cultures were grown in the presence of 5 mM glucose in shaken Erlenmeyer flasks while photoautotrophic cultures were routinely cultivated in U-tubes with air enriched by 1% CO_2. In some cases, 5 l flat-panel photo-bioreactors (KSD, Hattingen, Germany) were used for photoautotrophic growth. These cultures were illuminated either by white fluorescence light or by far red light provided by an array of high-power LEDs with a peak wavelength of 720 nm (ELD-720-524, Roithner Laser Technik, Vienna, Austria).

Chlorophyll determinations and absorption spectra

Chlorophyll (Chl) content of individual samples was determined according to (Porra 1989). Absorption spectra of cells were recorded in saturated sucrose solution using a Beckman DU 7400 spectrophotometer, with a baseline correction using white, light scattering media (few μl milk dissolved in 1 ml water) at the same OD_{750}.

Chlorophyll fluorescence measurements

Minimal (Fo) and variable (Fv) fluorescence values were obtained by recording fluorescence induction curves with a Dual-PAM-100 measuring system (Walz GmbH, Effeltrich, Germany) at 5 μg/ml Chl concentration. While Fo levels were determined in non-treated samples illuminated only by the weak (0.024 μE/m^2s) measuring beam, Fm (=Fo + Fv) levels were achieved by strong actinic light (I = 1,000 μE/m^2s) in the presence of 10 μM 3-(3′,4′-dichlorophenyl)-1, 1-dimethylurea (DCMU). Three to five independent samples were measured twice.

Oxygen evolution and consumption

Oxygen evolution and consumption were measured in 1 ml cell suspensions ([Chl] ≈ 5 μg/ml) of cultures in the exponential growth phase using a fiber-optic oxygenmeter (PreSens, Regensburg, Germany). Activities of the whole linear electron transport chain from water to CO_2 or fractions of it were investigated. For PS2 activity and $H_2O \rightarrow$ PS1 electron transport measurements, 500 μM 2,6-dichloro-benzoquinone (DCBQ) and 500 μM methyl viologen (MV), respectively, were used as electron acceptors. In some cases (see text) 10 μM carbonyl-cyanide m-chlorophenylhydrazone (CCCP) was used as uncoupling agent.

Photosynthetic rates and PS2 activities were determined as a difference of net oxygen evolution in light and oxygen consumption in the dark. Saturating red light (6,000 μE/m^2s) was provided by a KL 2500 LCD fiber optic halogen lamp (Schott, Mainz, Germany) in combination with a RG665 long pass filter. Oxygen consumption in presence of MV (Mehler reaction) was determined as difference of oxygen consumption in light and dark. Due to the low membrane permeability of MV, samples have been pre-incubated in the dark for 10 min prior to the measurements.

Low temperature fluorescence emission spectroscopy

Low temperature fluorescence emission spectra of cell suspensions were recorded by an Aminco-Bowman Series 2 luminescence spectrometer (SLM Spectronic Instruments, Rochester, NY) at 5 μg/ml Chl concentration. Excitation wavelengths of 440 and 580 nm were used for Chl and PBS excitation, respectively; excitation and emission bandwidths were set to 4 nm. Three individual traces of each sample were averaged, baseline-corrected, and smoothed by the instrumental software.

Measurement of "state transitions"

State transitions of WT and mutant cells were monitored by low temperature fluorescence emission measurements after PBS excitation as described above. In all the cases, a couple of identical samples were used. All the samples were first dark-incubated for 15 min to induce *State 2* as initial state. *State 1* was induced by a subsequent 15 min exposure to far red light (100 μE/m^2s) (Emlyn-Jones et al. 1999; Schluchter et al. 1996) generated by using an Omega BP700 interference filter. The illumination was performed in the thermostated sample holder of a home-built apparatus as in (Teuber et al. 2001). Samples in *State 1* and *2* were frozen in liquid nitrogen after the initial dark incubation and after the illumination, respectively. PS2/PS1 ratios of different strains were estimated by fluorescence emission spectra of *State 2* samples with Chl excitation.

P_{700} reduction kinetics and quantification of the linear and cyclic electron transport

Single trace P_{700} kinetic decays were recorded by a Dual-PAM-100 measuring system at 10 μg/ml Chl concentration. Complete P_{700} oxidation was achieved by a 100-ms saturation pulse (I = 10,000 μE/m^2 s). P_{700} reduction kinetics were recorded without any addition as well as in the presence of 10 μM DCMU and/or 500 μM MV, and fitted with single exponential functions; the resulting rate constants (k) were used for quantifying both the linear and the (direct) cyclic electron transport rates. Data were

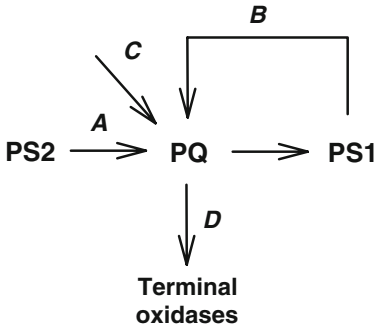

Fig. 1 Model used for the quantification of linear (A) and cyclic (B) electron flow based on P_{700} reduction kinetics measurements. See Fig. 6 and Materials and Methods for details

interpreted according to the model of Yu and coworkers (Yu et al. 1993) as modified by Yeremenko and coworkers (Yeremenko et al. 2005) (Fig. 1). The three main distinct routes for PQ-reduction, i.e., the linear, direct, and indirect cyclic electron transport routes, as well as the PQ re-oxidation by terminal oxidases are indicated by the letters A, B, C, and D, respectively. Note that routes B, C, and D consist (or may consist) of several parallel individual routes (Berry et al. 2002; Cooley and Vermaas 2001; Yeremenko et al. 2005).

The rate of linear and direct cyclic electron transport was quantified as a difference of rates as follows: k_1, the P_{700} reduction rate in non-treated samples, has a contribution from all the four major routes around PQ and can be expressed as

$$k_1 = k_A + k_B + k_C - k_D \quad (1)$$

where symbols k_A to k_D represent the individual routes on Fig. 1. In the presence of DCMU, route A is inactive and the decay follows the equation of

$$k_2 = k_B + k_C - k_D \quad (2)$$

Similar to this, route B is blocked by MV and the equation simplifies to

$$k_3 = k_A + k_C - k_D \quad (3)$$

In presence of both inhibitors, the decay represents the difference of the input rates from indirect cyclic route and respiration.

$$k_4 = k_C - k_D \quad (4)$$

Thus, linear and direct cyclic electron transport rates can be determined as

$$k_A = k_1 - k_2 = k_3 - k_4 \quad (5)$$

$$k_B = k_1 - k_3 = k_2 - k_4 \quad (6)$$

Calculation of k_A and k_B by the former or latter approach resulted in only minor differences. Note, that the "leak" contribution to the P_{700} reduction represents approximately 1% of the total electron flux (Yu et al. 1993) and was not incorporated into Eqs. 1–4. However, as such a contribution is eliminated by subtractions, taking it into account would result in the same values.

Results

Mutant phenotypes

ΔapcE, Olive, and PAL mutants, representing three distinct levels of antenna-deficiency in *Synechocystis* PCC 6803, differ by their phenotype. Most noticeably, their color is shifted from the natural blue-green of WT toward yellow: ΔapcE, Olive, and PAL have a characteristic yellowish green, olive green, and yellow color, respectively, as described previously (Shen et al. 1993; Ajlani and Vernotte 1998; Rögner et al. 1990). Absorption spectra of the mutants (Fig. 2) show differences in two regions. First, carotenoid absorption manifested as a shoulder around 490 nm is more pronounced if the antenna size is decreased. Second, the main PBS peak at 630 nm is highly reduced in Olive and PAL mutant. Although, due to spectral overlapping, distinct PBS-core absorption is not visible in the allophycocyanin (APC) containing strains, the local absorption minimum at 650 nm indicates that the central (core) light harvesting protein is also absent in the PAL mutant. The slight decrease of the PBS peak in the ΔapcE mutant indicates the reduced level of phycobilins in this mutant [see (Shen et al. 1993)].

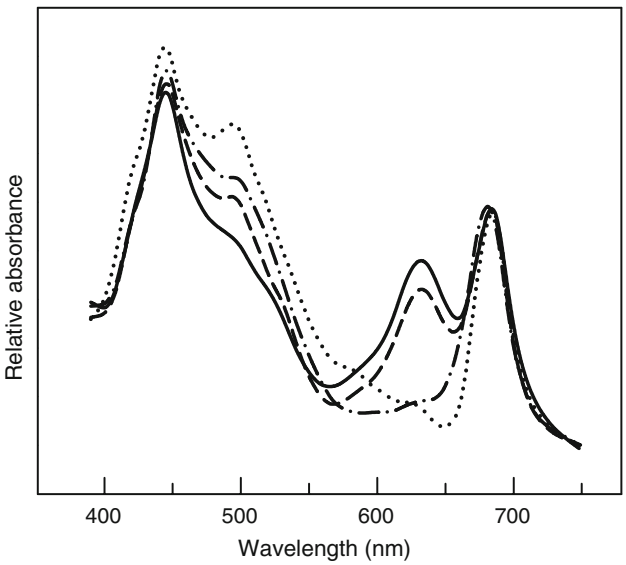

Fig. 2 Absorption spectra of WT and antenna-deficient *Synechocystis* PCC 6803 strains. Solid, dashed, dash-dotted, and dotted curves represent the spectra of WT, ΔapcE, Olive, and PAL strains, respectively. Spectra were corrected for light scattering and normalized to their 680 nm absorption peak

There are also considerable differences in the growth rates and the light-stress tolerance of WT and mutants: While ΔapcE and PAL grow 5–6 times slower than WT (which has a doubling time of 19.6 ± 6.2 h at 70 μE/m^{2}s light intensity) under photoautotrophic conditions (Ajlani and Vernotte 1998; Shen et al. 1993), the growth rate of Olive approximately doubles (doubling time 9.7 ± 0.3 h). Due to the diminished/missing PBS in the Olive and PAL mutants on the one hand and the decreased antenna-reaction center energy transfer in the ΔapcE strain on the other, the investigated antenna-deficient mutants are more resistant against photoinhibition (data not shown).

Energy transfer and short-term adaptation

Low temperature fluorescence emission spectra at PBS excitation (580 nm) confirm the absence of phycocyanin in the Olive and of both phycocyanin and allophycocyanin in the PAL mutant (Fig. 3). In WT cells (Fig. 3a), the peak at 665 nm and the shoulder at 650 nm indicate APC- and PC-emission, respectively. Corresponding peaks are missing in the PAL mutant (Fig. 3d) while the Olive mutant shows exclusively the APC peak (Fig. 3c). Peaks at 685/695 and 725 nm represent the energy transfer from PBS to PS2 and PS1, respectively. While shape and position of the PBS peaks are similar in ΔapcE mutant (Fig. 3b) and WT (Fig. 3a), their relative intensities are much higher in the mutant, indicating diminished energy transfer from PBS to the reaction center in absence of the L_{CM} linker protein.

In addition to severe changes in the energy transfer from phycobilisomes to the photosystems, Fig. 3 also indicates differences in the capability to perform state transitions, which play a very important role in the short-term adaptation of cells to changing light regimes. In contrast to higher plants, *Synechocystis* PCC 6803 is usually in *State 2* in darkness, as shown by the relative high PBS to PS1 energy transfer in the WT spectrum (Fig. 3a, solid line); this in turn is due to the dark reduction of the PQ pool by respiratory electron transport processes (Mao et al. 2002; Mullineaux and Allen 1986). Oxidation of the PQ pool by an illumination exciting preferably PS1 results in an increase in the PBS to PS2 energy transfer and "switches" the cells into *State 1* (Fig. 3a, dashed line). [In spite of analogies with higher plants the exact mechanism of state transition in cyanobacteria is still under debate, for reviews see (Mullineaux and Emlyn-Jones 2005; van Thor et al. 1998)]. While the Olive mutant—despite of a smaller antenna size—is still able to perform state transitions similar to WT (Fig. 3c), ΔapcE and PAL cells seem to have almost lost this capability (Fig. 3b and d).

Photosystem stoichiometry

Different from PBS excitation spectra which reflect mainly the energy transfer from PBS to PS1 and PS2 (Fig. 3 with the exception of the PAL mutant which has no PBS), Chl excitation (i.e. 440 nm) induces fluorescence emission of the photosystems directly. For various photosynthetic

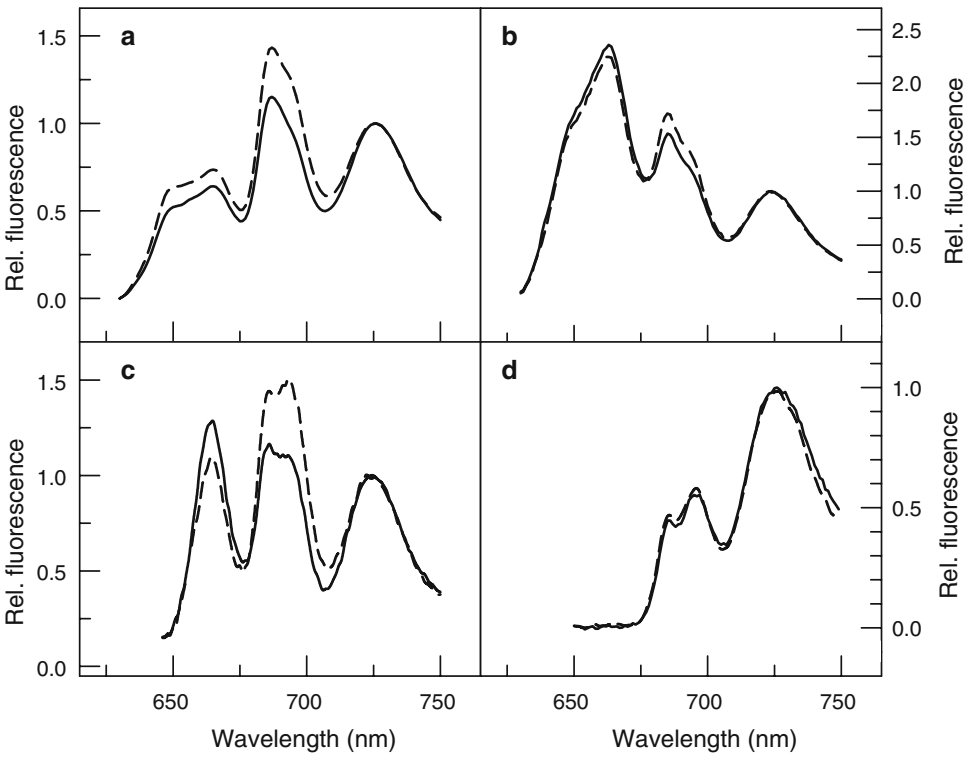

Fig. 3 Low temperature (77 K) fluorescence spectra of photoautotrophically grown wild type (**a**), ΔapcE (**b**), Olive (**c**), and PAL (**d**) mutant of *Synechocystis* PCC 6803 at an excitation wavelength of 580 nm. Solid and dashed curves represent two parallel samples which have been frozen after 15 min dark incubation and after a subsequent far red illumination, respectively. All curves were normalized to the emission peak at 725 nm

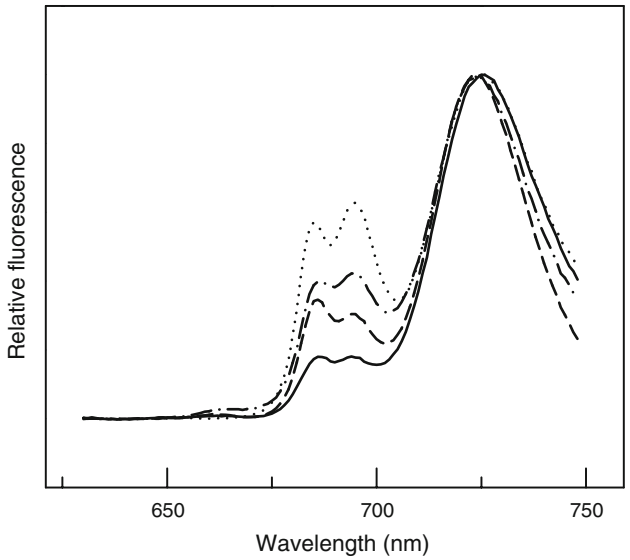

Fig. 4 Low temperature (77 K) fluorescence spectra (excitation wavelength = 440 nm) from *Synechocystis* cells grown photoautotrophically at low light (45 μE/m^{2}s). Solid, dashed, dash-dotted, and dotted curves represent the spectra of WT, ΔapcE, Olive, and PAL strains, respectively. Samples were frozen after 15 min of dark incubation. All curves were normalized to the PS1 emission peak at 725 nm

organisms ranging from cyanobacteria to higher plants, a quantitative linear relationship between PS1/PS2 fluorescence and the molar ratio between the photosystems has been observed (Murakami 1997). Thereby, the ratio of the peak intensities at 685/695 nm relative to 725 nm provide a rough estimation on the PS2/PS1 ratio. While higher plants routinely show a PS2/PS1-ratio around 1, *Synechocystis* WT contains 5–6 times more PS1 than PS2 (Fig. 4, solid line). (For this reason, the PQ pool can easily be oxidized by illumination after dark incubation.) Figure 4 shows that PBS-antenna deficiency results in a higher PS2/PS1 fluorescence (corresponding with molar) ratio which increases by a factor of 1.9 for ΔapcE-, 2.4 for Olive, and 3.6 for the PAL mutant relative to WT. The same tendency was found by fluorescence induction measurements with variable fluorescence component (Fv) originating from PS2 and minimal fluorescence (Fo) containing emissions also from PBS (Campbell et al. 1998) and PS1 (Franck et al. 2002). While WT samples show Fv/Fo ratios of 0.508 ± 0.007, corresponding values in Olive and PAL mutant are 1.646 ± 0.029 and 1.770 ± 0.066, respectively (data not shown); these 3.2- and 3.5-fold higher values also clearly reflect an increasing PS2/PS1 ratio.

Linear and cyclic electron transport activity

In order to test the assumption that a higher PS2/PS1 ratio is correlated with a higher maximal electron transport rate, different parts of the linear electron transport chain were tested (Fig. 5). In agreement with the low-temperature (Fig. 4) and room-temperature Chl-fluorescence results, oxygen evolving activity of PS2 determined in presence of DCBQ as electron acceptor increased relative to WT in the sequence ΔapcE, Olive, and PAL strain (Fig. 5a). Remarkably, photoautotrophically grown cultures (Fig. 5a, right) show about 1.5-fold higher PS2 activities than cultures grown mixotrophically (Fig. 5a, left). Higher PS2 activity is a necessary but not sufficient requirement for our purpose: A higher electron flow in the linear electron transport chain is also required. Therefore, the overall linear electron transport rate from water to bicarbonate or from water to MV provides more direct information on the potential H_2-evolution capacity by antenna-deficient *Synechocystis* mutants. Figure 5b and c show a significant decrease in the maximal electron flux relative to Fig. 5a due to the time-consuming and rate-limiting steps between PS2 and the terminal electron acceptors (HCO_3^- or MV), in contrast to the "fast" electron transport through PS2. Figure 5b (left) shows increased electron transport from H_2O to HCO_3^- with decreasing antenna size in mixotrophic cultures. Under these conditions, photoautotrophically grown cultures did not show a clear tendency (Fig. 5b, right). In order to test whether this reflects the rate limitation of Ribulose-1,5-biphosphate carboxylase/oxygenase (Rubisco), MV was used as an alternative electron acceptor of PS1 (Fig. 5c) resulting in the highest activity of Olive and PAL mutant under both mixotrophic and photoautotrophic conditions, respectively. (As H_2-ase enzymes take up electrons from the PS1 acceptor side, the use of MV could mimic the competition of H_2-ase for electrons which transported by the linear electron transport chain.) However, due to the possible net electron input or output by the reductive and oxidative respiratory electron transport chain(s), respectively, some uncertainty in the linear electron transport activity with MV acceptor should be considered. [In the linear electron transport chain, evolution of one molecule O_2 at the oxygen-evolving complex of PS2 (OEC) is accompanied with the donation of four electrons; these four electrons reduce finally two molecules of O_2 (to H_2O_2) at MV. Therefore, without respiration, the absolute value of the net O_2 consumption (−1/4 molecule O_2 per electron) would equal with the rate of O_2^-evolution (+1/4 O_2 per e^-) at the OEC.] As re-oxidation and deprotonation of PQH_2, occurring at the Q_o site of the Cyt b_6f complex, is one of the rate limiting steps in photosynthetic electron transport and is also highly dependent on the electrochemical proton gradient (McCauley et al. 1987), the use of uncouplers should increase the linear electron transport rate. Figure 5c left (striped columns) shows an about 2-fold increase with the uncoupler CCCP under mixotrophic conditions both in the cases of Olive and PAL, although Olive showed about twice as high absolute activities than PAL.

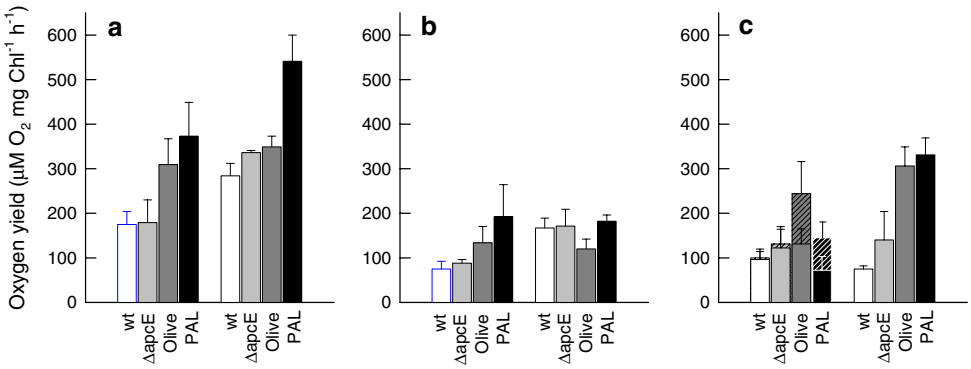

Fig. 5 Comparison of the linear electron transport activity from *Synechocystis* WT and mutant strains by oxygen evolution and oxygen consumption experiments: (**a**) PS2 activity in the presence with DCBQ, (**b**) linear electron transport from H_2O to HCO_3^-, and (**c**) from H_2O to MV (for details see Materials and Methods). Panels *a* and *b* indicate net oxygen evolution, panel *c* net oxygen consumption (difference of O_2 consumption by the Mehler-reaction at PS1 and oxygen evolution at PS2). Left and right columns on each panel represent values from mixotrophic and photoautotrophic cultures, respectively; the striped columns on panel *c* show oxygen consumption in the presence of the protonophore CCCP. Each electron transport activity represents the average of 5–7 independent cultures with error bars indicating the standard deviation

The accurate quantification of linear electron transport activities by O_2-measurements is severely hampered by the facts that direct and indirect cyclic electron transport(s) feed electrons into the linear electron transport chain, and (oxidative) respiratory routes extract electrons from it. Furthermore, these measurements provide no information about the cyclic electron transport. In order to quantify linear and cyclic electron flow, P_{700} reduction kinetics after saturating light pulses were recorded in non-treated samples as well as under conditions where linear and/or (direct) cyclic electron transport were blocked. While Fig. 6a shows the principle of these measurements, Fig. 6b and c summarize the determined rates (for details see Materials and Methods and Fig. 1). Figure 6b and c show the overall as well as individual linear and cyclic electron transport activities as deduced from the P_{700} reduction rates in mixotrophically and autotrophically grown cultures, respectively. While mixotrophic cultures show a high contribution of the cyclic electron transport to the P_{700} reduction kinetics, photoautotrophic cultures are dominated by the linear route. In addition, Fig. 6c shows that both overall and linear electron transport increases with decreasing antenna size (i.e., with a higher PS2 population) when cells are grown autotrophically. The overall (cyclic + linear) activity increases in the ΔapcE, Olive, and PAL strain by a factor of 1.8, 3.7, and 4.7, respectively, relative to WT. The individual linear and cyclic electron rates increased proportionally (1.8 and 3.7 fold) in ΔapcE and in Olive mutant. However, while the linear activity increased 5.5-fold in the PAL mutant, its cyclic electron rate was identical to WT, indicating a very low contribution of the cyclic electron transport to the P_{700} reduction (and to the overall electron flux) in this strain.

Long-term adaptation and light quality

In contrast to short-term adaptation processes such as state transitions which respond to changes of light quantity and quality in a minute time range (see the review of Finazzi and coworkers in this issue), adjustment of the PS2/PS1 ratio requires more time. Figure 7 shows the effect of light quantity and quality on the PS2/PS1 ratio in WT, Olive, and PAL mutant. An increase of the (white) light intensity from 45 to 100 μE/m^{2}s resulted in an about 20% increase of PS2 relative to PS1 in WT, Olive, and PAL mutant (compare solid lines of Fig. 7 with the respective PS2/PS1 fluorescence ratios of Fig. 4). An additional increase of the PS2/PS1 ratio could be achieved by illumination with 720 nm (PS1) light (Fig. 7a–c, dashed lines). While in the Olive strain the PS2/PS1 fluorescence ratio increased from 0.42 (under strong white light) to 0.63 (under far red light), the corresponding ratio increased in the PAL mutant from 0.87 to 1.08, i.e., close to the (1:1) ratio usually found in higher plants and green algae.

Discussion

As mentioned before, the following parameters have to be optimized in a cell designed for maximum hydrogen production with electrons originating from the terminal electron donor water:

a) the absolute amount of PS2 and the (relative) PS2/PS1 ratio
b) the absolute rate of the linear electron transport as well as the linear/cyclic electron transport ratio
c) the amount of antenna pigments in relation to the potential cell density in mass cultures

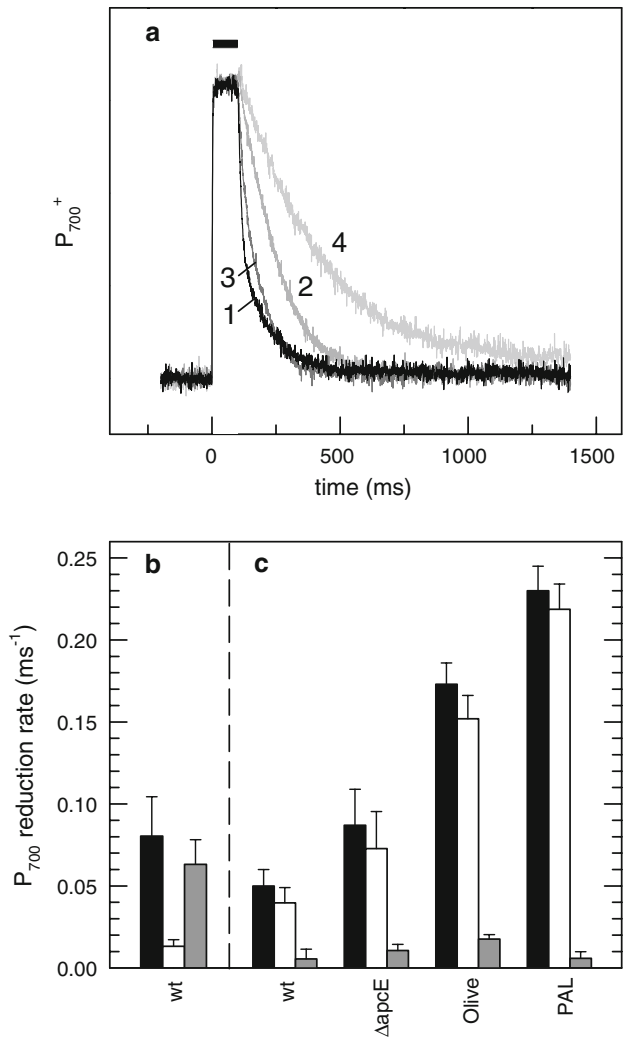

Fig. 6 Quantification of linear and cyclic electron transport from P_{700} reduction kinetics measurements. As an example, panel *a* shows the experimental curve set for a WT sample. The black rectangle over the traces indicates the time interval of the saturating pulse (100 ms), which is followed by the (dark) reduction of P_{700}: This is fastest in the untreated sample (curve 1) and slowed down in presence of DCMU (curve 2) and/or MV (curves 3 and 4) due to blocked linear and/or cyclic route(s), respectively. Corresponding rate constants were determined by fitting with single exponential functions. Individual rate constants of linear and cyclic electron transport (panels *b* and *c*) represent the difference of such experimental rate constants (for details, see Materials and Methods). Panel *b* and *c* show results with mixotrophic and photoautotrophic cultures, respectively, with black, white, and gray columns representing the calculated overall, linear and cyclic activities. Electron transport rates represent the mean values of 3–5 independent cultures with error bars indicating the standard deviation

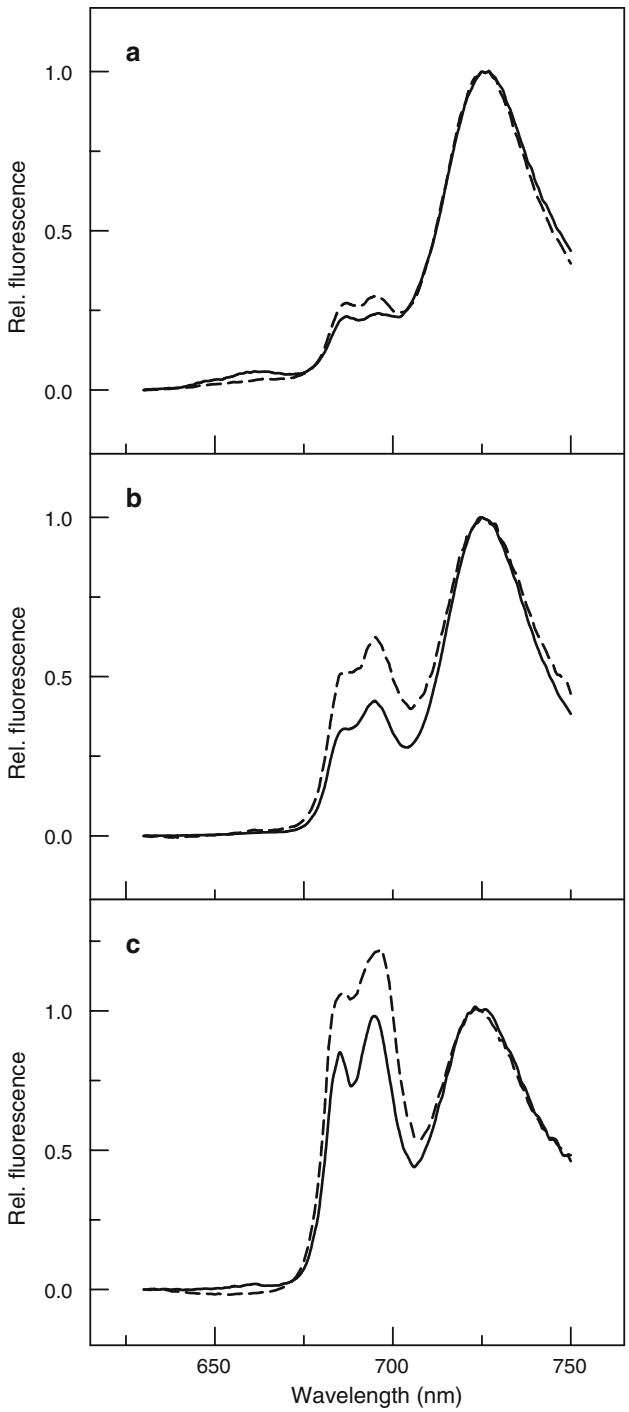

Fig. 7 Low temperature (77 K) fluorescence emission spectra of photoautotrophic *Synechocystis* cultures grown under 100 $\mu E/m^2 s$ white (solid lines) or far red (dashed lines) light. Excitation wavelength was 440 nm. Spectra of WT, Olive, and PAL strains are shown on panel *a*, *b*, and *c*, respectively. Samples were frozen after 15-min dark incubation. All curves were normalized to the PS1 emission peak at 725 nm

Results obtained in this article are based on three mutants with various degrees of phycobilisome antenna reduction. It could be shown that they have impact both on dynamic (i.e., state transitions) and "static" aspects of electron transport (i.e., the PS2/PS1 ratio) which also have to be discussed in combination with environment-induced adaptations (i.e., photo-autotrophic and mixotrophic growth conditions, light regime, etc.). Having in mind to use one or the other of these mutants as starting material for

a further iterative process toward water-splitting-based hydrogen production, the results are discussed with special focus on this future goal.

Potentially higher H_2-production by upregulation of the PS2/PS1 ratio

Although cyanobacteria seem to be ideal organisms for producing molecular hydrogen with respect to biotechnology and genetic manipulation, their low PS2/PS1 ratio is one of the key problems. In contrast to higher plants and green algae with a PS2/PS1 ratio of about 1:1, the evolutionary adaptation of cyanobacteria to their environment resulted in a much lower ratio (see Fujita and Murakami 1987). In consequence, most of the absorbed light energy is used for cyclic electron transport, especially under mixotrophic conditions, and the yield of net electron flow (from water), i.e., the linear electron transport which potentially may be used for hydrogen production beyond PS1, is low. Fortunately, the PS2/PS1 ratio is tunable, as it is affected by many environmental (light quality, nutrient composition) and physiological parameters. Results of Fujita and Murakami (1987) obtained with *Synechocystis* PCC 6714 cells indicated a higher PS2/PS1 ratio when their linear electron transport was up-regulated. In line with this, our observations with *Synechocystis* PCC 6803 show that a reduced or missing phycobilisome antenna, photoautotrophic growth conditions, and illumination with far red (PS1) light all result in an increased PS2 population and increased linear electron transport. The combination of these factors (see. Fig. 7) probably will contribute to a potentially very high H_2-production rate.

The decreased PBS antenna size (PS2 cross-section decrease) is overcompensated by the increased PS2 population size resulting in higher linear electron transport activities. Physiologically, the ability to modulate the PS2/PS1 ratio in higher plants and cyanobacteria helps to maintain efficient light energy utilization and to minimize damage caused by light stress. While the observed high PS2/PS1 ratios could be either due to an increased PS2 or a decreased PS1 pool (or both), published data strongly suggest a regulation *via* control of the abundant PS1 (Fujimori et al. 2005; Herranen et al. 2005; Sonoike et al. 2001), i.e., the antenna-deficient mutants, especially Olive and PAL, most probably contain a constant PS2 and a decreased PS1 population size. However, due to the higher maximal cell density of the mutant strains (see below), their absolute PS2 concentration is higher than in WT. Despite extensive studies, the molecular mechanism of this photosystem modulation is still poorly understood; however, there are indications that the redox level of certain components of the electron transport chain plays a crucial role (Pfannschmidt et al. 2001). The model of Sonoike and co-workers (Sonoike et al. 2001) suggests, that the main role of downregulated PS1 synthesis under high light is to avoid the formation of reactive oxygen species which are produced by the high (cyclic) electron transport. In this context, the smaller PBS antenna size of the mutants, which in turn results in a more oxidized PQ pool (due to less efficient light-energy utilization), could initiate the same regulatory processes as high light does in WT cultures. The upregulated carotenoid content (Fig. 2), which is thought to protect organisms against light stress supports this idea (Bonente et al. 2008).

Increase of linear electron transport rate and linear/cyclic electron transport ratio

All electrons participating in the electron transport processes either earlier or later originate from the terminal electron donor water. As there is no net electron production in the cyclic electron transport, linear electron flow has to be upregulated in order to achieve a maximal H_2-production rate. Antenna-deficient mutants display higher PS2/PS1 ratios (Fig. 4), which involve higher linear electron transport activity (Figs. 5 and 6). The highest PS2/PS1 ratios have been observed in the PC- and PBS-depleted Olive and PAL mutant, respectively. With these, maximal linear electron flow can be achieved by the optimization of certain abiotic parameters, such as the composition of growth media (photoautotrophic growth, Figs. 5 and 6), the presence of protonophores (Fig. 5) and adjustment of light quality and quantity (Figs. 4 and 7). Surprisingly, downregulation of the cyclic is not a prerequisite for the upregulation of the linear electron transport. Rather, both seem to increase proportionally in ΔapcE and Olive strain. In contrast, contribution of the cyclic electron transport is quite low in the PAL mutant (Fig. 6), which also shows a rather slow growth in comparison with WT and Olive strain. Possibly, the parallel increase of cyclic and linear electron transport in the Olive mutant, which is lacking in the PAL mutant, is the prerequisite for higher growth rates. This view may be supported by the fact, that one key component of the direct cyclic transport, the ferredoxin:$NADP^+$ oxidoreductase (FNR) apparently binds to the PBS rods via its linker domain (Gomez-Lojero et al. 2003; van Thor et al. 1999). FNR binding to the APC core has been also reported (van Thor et al. 1999). In conclusion, the observed low cyclic activity of the PAL mutant could be correlated with the missing FNR binding site close to the membrane, which in turn is necessary for the cyclic electron transport.

In terms of future hydrogen production, growth under photoautotrophic conditions which strongly favors linear electron transport is rather an advantage, as future mass cultures in photobioreactors will be considerably cheaper if

they do not have to be supplemented by glucose or other (bio)organic nutrients.

Potential H_2-production by antenna-deficient *Synechocystis* PCC 6803

In the framework of our results, a crude estimation of potential future hydrogen production rates using the most appropriate strains of our investigation, i.e., Olive, and PAL mutant, seems worthwhile. The decreased or missing PBS antenna would be disadvantageous under natural conditions when light is a limiting factor. However, as pointed out by Polle and coworkers (2002) the antenna absorbs under bright (sun)light far more photons than photosynthesis can utilize, i.e., most of the photons are dissipated as fluorescence or heat and, therefore, lost for instance for biomass and biofuel production. In addition, especially WT cultures at high cell densities absorb most of the light in a thin layer at the surface due to their high antenna pigment concentrations, while deeper layers are lacking light due to the self-shading effect of the cells, i.e., most of the cells grow light-limited. For this reason, strains with reduced antenna size are preferable for photo-biological H_2-production under mass fermentation conditions. First, their energy conversion and productivity is more efficient due to their smaller antenna size (less energy lost). Also, owing to the lower absorbance of the cells, light can easily penetrate into deeper layers resulting in higher cell densities (combined with potentially higher H_2 production rates) of the cultures. This is reflected by the Chl concentration of the four strains from our study: At the stationary phase, WT and ΔapcE culture achieved around 20 μg Chl/ml, while Olive and PAL mutant yielded at least the double concentration (data not shown). Not incidentally, these antenna-deficient strains are also more resistant against light stress and need less energy for (PS2) repair after photodamage and antenna synthesis. The considerably higher linear electron flows in these mutants (as shown above) has then to be directed from PS1 to a heterologously expressed H_2-ase with high turnover rate and which previously will have been engineered for oxygen tolerance. Concomitantly, the electron flow for CO_2 fixation has to be minimized. Assuming a positive outcome of these certainly challenging future experiments, the following estimations can be made.

By combination of the data obtained from oxygen evolution- (Fig. 5) and P_{700} reduction kinetics measurements (Fig. 6) as well as the achievable optical cell densities, some conclusions concerning the potential rate of H_2 evolution can be drawn. Assuming continuous cultures of Olive or PAL mutant, which stabilize them in the exponential phase (20 μg Chl/ml), and considering an O_2 production rate of 300 μM O_2/mg Chl h (Fig. 5), with 75% of the linear electrons being used for H_2-production (and 25% for CO_2 fixation), this would result in approximately 200 ml H_2/h by a 1 l culture (using uncouplers, this number could be even higher). This rate exceeds the highest up to now published H_2-production rate, which was achieved with *Chlamydomonas* cultures under sulfur deprivation (Melis et al. 2000), by a factor of about 100! Independently, the potential H_2 production rate can also be estimated from the P_{700} reduction kinetics for both mutants (175 and 220 turnovers per seconds for Olive and PAL mutant, respectively). Considering a (theoretical) minimum of five electrons for the production of one molecule H_2 (Melis and Happe 2001), we gain 230 and 290 ml H_2/h, respectively, which is in agreement with the previous approach.

In summary, our results show that the combination of appropriate antenna mutants and optimized environmental conditions (growth media composition, light quality, and quantity) considerably upregulates linear electron transport, which in turn is a prerequisite for achieving high photosynthesis-based hydrogen production yields. Among the tested strains, both Olive and PAL mutant are especially well suited for this purpose based on their biophysical properties. Oxygen and electron transport rates determined in these mutants allow a quantitative estimation of potential hydrogen production rates in a best-case scenario. In parallel, the direct comparison of WT and mutants under ambient conditions allows to draw conclusions about the molecular-level strategies of these cells which enable them to adopt and survive under different (e.g., stress) environmental conditions. This step-by-step understanding of physiological responses of whole organisms and the management of its predictability is the prerequisite for designing cells for future needs—such as energy production.

Acknowledgments The financial supports by the Federal Ministry of Education and Research (BMBF, project "Bio-H_2"), the EU/NEST project "Solar-H", and the German Research Foundation (DFG, project C1 in SFB 480) are gratefully acknowledged. We thank Erdmut Thomas for excellent technical assistance, and Anna Sallai, Regina Oworah-Nkruma, and Daichi Takenaka for their help with the strains. The PAL mutant was a kind gift from Ghada Ajlani and Zoltán Gombos; fruitful discussion with the latter is also much appreciated.

References

Ajlani G, Vernotte C (1998) Construction and characterization of a phycobiliprotein-less mutant of Synechocystis sp. PCC 6803. Plant Mol Biol 37:577–580. doi:10.1023/A:1005924730298

Berry S, Schneider D, Vermaas WFJ, Rögner M (2002) Electron transport routes in whole cells of Synechocystis sp strain PCC 6803: the role of the cytochrome bd-type oxidase. Biochemistry 41:3422–3429. doi:10.1021/bi011683d

Bonente G, Dall'Osto L, Bassi R (2008) In between photosynthesis and photoinhibition: the fundamental role of carotenoids and carotenoid-binding proteins in photoprotection. In: Pavesi L,

Fauchet PM (eds) Biophotonics. Springer, New York, NY, pp 29–46

Campbell D, Hurry V, Clarke AK, Gustafsson P, Öquist G (1998) Chlorophyll fluorescence analysis of cyanobacterial photosynthesis and acclimation. Microbiol Mol Biol Rev 62:667–683

Cooley JW, Vermaas WFJ (2001) Succinate dehydrogenase and other respiratory pathways in thylakoid membranes of Synechocystis sp strain PCC 6803: capacity comparisons and physiological function. J Bacteriol 183:4251–4258. doi:10.1128/JB.183.14.4251-4258.2001

Emlyn-Jones D, Ashby MK, Mullineaux CW (1999) A gene required for the regulation of photosynthetic light harvesting in the cyanobacterium Synechocystis 6803. Mol Microbiol 33:1050–1058. doi:10.1046/j.1365-2958.1999.01547.x

Esper B, Badura A, Rögner M (2006) Photosynthesis as a power supply for (bio-)hydrogen production. Trends Plant Sci 11:543–549. doi:10.1016/j.tplants.2006.09.001

Franck F, Juneau P, Popovic R (2002) Resolution of the Photosystem I and Photosystem II contributions to chlorophyll fluorescence of intact leaves at room temperature. Biochim Biophys Acta 1556:239–246. doi:10.1016/S0005-2728(02)00366-3

Fujimori T, Higuchi M, Sato H, Aiba H, Muramatsu M, Hihara Y, Sonoike K (2005) The mutant of sll1961, which encodes a putative transcriptional regulator, has a defect in regulation of photosystem stoichiometry in the cyanobacterium Synechocystis sp PCC 6803. Plant Physiol 139:408–416. doi:10.1104/pp.105.064782

Fujita Y, Murakami A (1987) Regulation of electron-transport composition in cyanobacterial photosynthetic system—stoichiometry among Photosystem-I and Photosystem-II complexes and their light-harvesting antennae and Cytochrome-b6 Cytochrome-f complex. Plant Cell Physiol 28:1547–1553

Fujita Y, Murakami A, Aizawa K, Ohki K (1994) Short-term and long-term adaptation of the photosynthetic apparatus: homeostatic properties of thylakoids. In: Bryant DA (ed) The molecular biology of cyanobacteria. Kluwer Academic Publishers, Dordrecht, The Nederlands, pp 677–692

Ghirardi ML, Posewitz MC, Maness PC, Dubini A, Yu JP, Seibert M (2007) Hydrogenases and hydrogen photoproduction in oxygenic photosynthetic organisms. Annu Rev Plant Biol 58:71–91. doi:10.1146/annurev.arplant.58.032806.103848

Gomez-Lojero C, Perez-Gomez B, Shen GZ, Schluchter WM, Bryant DA (2003) Interaction of ferredoxin : NADP(+) oxidoreductase with phycobilisomes and phycobilisome substructures of the cyanobacterium Synechococcus sp strain PCC 7002. Biochemistry 42:13800–13811. doi:10.1021/bi0346998

Herranen M, Tyystjärvi T, Aro EM (2005) Regulation of photosystem I reaction center genes in Synechocystis sp strain PCC 6803 during light acclimation. Plant Cell Physiol 46:1484–1493. doi:10.1093/pcp/pci160

Kondo K, Ochiai Y, Katayama M, Ikeuchi M (2007) The membrane-associated CpcG2-phycobilisome in Synechocystis: a new photosystem I antenna. Plant Physiol 144:1200–1210. doi:10.1104/pp.107.099267

Kruse O, Rupprecht J, Bader KP, Thomas-Hall S, Schenk PM, Finazzi G, Hankamer B (2005) Improved photobiological H-2 production in engineered green algal cells. J Biol Chem 280:34170–34177. doi:10.1074/jbc.M503840200

Leong TY, Anderson JM (1986) Light-quality and irradiance adaptation of the composition and function of pea-thylakoid membranes. Biochim Biophys Acta 850:57–63. doi:10.1016/0005-2728(86)90008-3

Mao HB, Li GF, Ruan X, Wu QY, Gong YD, Zhang XF, Zhao NM (2002) The redox state of plastoquinone pool regulates state transitions via cytochrome b(6)f complex in Synechocystis sp PCC 6803. FEBS Lett 519:82–86. doi:10.1016/S0014-5793(02)02715-1

McCauley SW, Melis A, Tang GMS, Arnon DI (1987) Protonophores induce plastoquinol oxidation and quench chloroplast fluorescence—evidence for a cyclic, proton-conducting pathway in oxygenic photosynthesis. Proc Natl Acad Sci USA 84:8424–8428. doi:10.1073/pnas.84.23.8424

Melis A, Happe T (2001) Hydrogen production. Green algae as a source of energy. Plant Physiol 127:740–748. doi:10.1104/pp.010498

Melis A, Zhang LP, Forestier M, Ghirardi ML, Seibert M (2000) Sustained photobiological hydrogen gas production upon reversible inactivation of oxygen evolution in the green alga Chlamydomonas reinhardtii. Plant Physiol 122:127–135. doi:10.1104/pp.122.1.127

Mullineaux CW, Allen JF (1986) The State-2 transition in the cyanobacterium Synechococcus-6301 can be driven by respiratory electron flow into the plastoquinone pool. FEBS Lett 205:155–160. doi:10.1016/0014-5793(86)80885-7

Mullineaux CW, Emlyn-Jones D (2005) State transitions: an example of acclimation to low-light stress. J Exp Bot 56:389–393. doi:10.1093/jxb/eri064

Murakami A (1997) Quantitative analysis of 77 K fluorescence emission spectra in Synechocystis sp. PCC 6714 and *Chlamydomonas reinhardtii* with variable PS I/PS II stoichiometries. Photosynth Res 53:141–148. doi:10.1023/A:1005818317797

Ozaki H, Ikeuchi M, Ogawa T, Fukuzawa H, Sonoike K (2007) Large-scale analysis of chlorophyll fluorescence kinetics in Synechocystis sp PCC 6803: identification of the factors involved in the modulation of photosystem stoichiometry. Plant Cell Physiol 48:451–458. doi:10.1093/pcp/pcm015

Pfannschmidt T, Schütze K, Brost M, Oelmüller R (2001) A novel mechanism of nuclear photosynthesis gene regulation by redox signals from the chloroplast during photosystem stoichiometry adjustment. J Biol Chem 276:36125–36130. doi:10.1074/jbc.M105701200

Polle JEW, Kanakagiri S, Jin E, Masuda T, Melis A (2002) Truncated chlorophyll antenna size of the photosystems—a practical method to improve microalgal productivity and hydrogen production in mass culture. Int J Hydrogen Energy 27:1257–1264. doi:10.1016/S0360-3199(02)00116-7

Porra RJ, Thompson WA, Kriedmann PE (1989) Determination of accurate extinction coefficients and simultaneous equations for assaying chlorophylls a and b extracted with four different solvents: verification of the concentrations of chlorophyll standards by atomic absorption spectroscopy. Biochim Biophys Acta 975:384–394. doi:10.1016/S0005-2728(89)80347-0

Rögner M, Nixon P, Diner B (1990) Purification and characterization of photosystem I and photosystem II core complexes from wild-type and phycocyanin-deficient strains of the cyanobacterium Synechocystis PCC 6803. J Biol Chem 265:6189–6196

Schluchter WM, Shen G, Zhao J, Bryant DA (1996) Characterization of psaI, psaL mutants of Synechococcus sp. strain PCC 7002: a new model for state transitions in cyanobacteria. Photochem Photobiol 64:53–66. doi:10.1111/j.1751-1097.1996.tb02421.x

Shen G, Boussiba S, Vermaas WF (1993) Synechocystis sp PCC 6803 strains lacking photosystem I and phycobilisome function. Plant Cell 5:1853–1863

Sonoike K, Hihara Y, Ikeuchi M (2001) Physiological significance of the regulation of photosystem stoichiometry upon high light acclimation of Synechocystis sp PCC 6803. Plant Cell Physiol 42:379–384. doi:10.1093/pcp/pce046

Teuber M, Rögner M, Berry S (2001) Fluorescent probes for non-invasive bioenergetic studies of whole cyanobacterial cells. Biochim Biophys Acta 1506:31–46. doi:10.1016/S0005-2728(01)00178-5

van Thor JJ, Gruters OW, Matthijs HC, Hellingwerf KJ (1999) Localization and function of ferredoxin:NADP(+) reductase

bound to the phycobilisomes of Synechocystis. EMBO J 18:4128–4136. doi:10.1093/emboj/18.15.4128

van Thor JJ, Mullineaux CW, Matthijs HCP, Hellingwerf KJ (1998) Light harvesting and state transitions in cyanobacteria. Bot Acta 111:430–443

Vignais PM, Billoud B (2007) Occurrence, classification, and biological function of hydrogenases: an overview. Chem Rev 107:4206–4272. doi:10.1021/cr050196r

Yeremenko N, Jeanjean R, Prommeenate P, Krasikov V, Nixon PJ, Vermaas WFJ, Havaux M, Matthijs HCP (2005) Open reading frame ssr2016 is required for antimycin A-sensitive photosystem I-driven cyclic electron flow in the cyanobacterium Synechocystis sp PCC 6803. Plant Cell Physiol 46:1433–1436. doi:10.1093/pcp/pci147

Yu L, Zhao JD, Mühlenhoff U, Bryant DA, Golbeck JH (1993) Psae is required for in-vivo cyclic electron flow around Photosystem-I in the cyanobacterium Synechococcus sp-Pcc-7002. Plant Physiol 103:171–180